Chapter 2 Assignment of ^{13}C, ^{15}N and ^{1}H signals of proteins by solid-state MAS NMR

2.1 Introduction

For investigations of proteins by either solution or solid-state NMR spectroscopy, the resonance assignment of the individual sites of the system is mandatory. Assignment means to correlate the correct chemical shift of the observed resonances to each individual spin. In solution NMR, multidimensional homonuclear and heteronuclear chemical shift correlation methods are based on scalar couplings to transfer the coherence between spins, and provide a basis for the resonance assignment of proteins[1-6]. Nowadays, assignment and subsequent structure determination of fully ^{13}C,^{15}N-labelled proteins of up to 50 kDa is common practice in the liquid-state, and recent developments have extended in certain cases this boundary to about 500 kDa[7]. Analogous correlation schemes can be employed in designing multidimensional MAS experiments for resonance assignment of solid proteins. The advantage in utilizing MAS methods is that the observed isotropic shift allows the identification of the different amino-acid types by means of the characteristic side-chain correlation patterns, as in solution NMR. Different from solution NMR, however, is that in the solid-state one does not only use scalar couplings but also dipolar couplings for coherence transfer. Under MAS, homonuclear and heteronuclear dipolar couplings can be reintroduced by various radio-frequency sequences[8-15]. Another main difference between the two techniques lays in the type of spins generally used for observation. In solution NMR, assignment experiments, such as CBCACONNH or CBCANNH, all involve proton detection. In solid-state NMR ^{1}H detection is generally not feasible, because of the strong dipolar couplings between protons, which give rise to broad lines, even when using sophisticated

resolution enhancement techniques[16-19] combined with fast magic-angle sample spinning in the highest possible magnetic fields. Since low-γ nuclei, such as ^{13}C and ^{15}N, have smaller dipolar couplings and a larger chemical shift range, they give rise to much better resolved spectra and are the nuclei of choice for detection. A potential assignment strategy for solid-state applications involves ^{13}C and ^{15}N signals and consists of two main steps. It starts with the identification of the ^{13}C resonances belonging to the same amino-acid residue, upon characteristic correlation patterns in homonuclear dipolar ^{13}C correlation spectra[20-24]. The second step concerns the sequential assignment, that is accomplished using selective transfer between the ^{15}N backbone signals and the C^{α} and CO signals, to connect one residue of the protein chain to the next and previous one[13,22-26]. For the latter step, different ^{15}N-^{13}C heteronuclear correlation experiments have been proposed, based on frequency selective ^{15}N-^{13}C cross polarization[27] or dipolar recoupling techniques, such as REDOR[28]. This two-step strategy has been applied to obtain an almost full ^{15}N,^{13}C solid-state resonance assignment for the α-spectrin SH3 domain[22], and is described in more details in the following section. Once the ^{13}C and ^{15}N assignment is completed, the assignment of the proton resonances can be achieved by multi-dimensional NMR spectroscopy, taking advantage of the greater resolution in the $^{13}C/^{15}N$ dimension. In section 2.3, the assignment of the proton resonances of the SH3 is presented.

2.2 Backbone and side-chain ^{13}C and ^{15}N resonance assignment

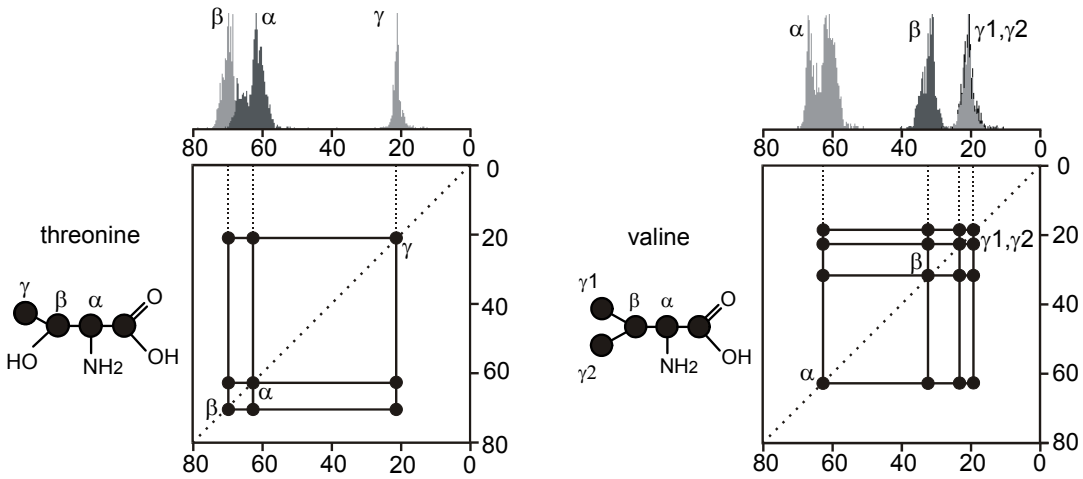

Fig. 2.1 Characteristic intra-residue correlation patterns in the case of a threonine (left) and a valine residue (right), together with the statistical distributions of the aliphatic carbon chemical shifts, obtained from the BioMagResBank database.

In the first step of the resonance assignment procedure, ^{13}C homonuclear correlation experiments are recorded on uniformly labelled proteins. In these spectra, amino-acid side-chains can be identified, due to characteristic correlation patterns formed by correlated peaks, which resonate in well-defined regions of the spectrum. In Fig. 2.1 schematic representations of the correlation patterns obtained in the case of threonine and valine residues are shown. In the figure is also reported the statistics on ^{13}C chemical shifts derived by studies of proteins in solution (*http://www.bmrb.wisc.edu/*), and can be used as a guide for the identification of the different amino-acid networks. In Fig. 2.2 a 2D ^{13}C homonuclear correlation spectrum is shown, recorded on a fully ^{13}C,^{15}N-enriched SH3 domain using the radio-frequency-driven dipolar recoupling (RFDR) sequence[8] with a mixing time of 3 ms.

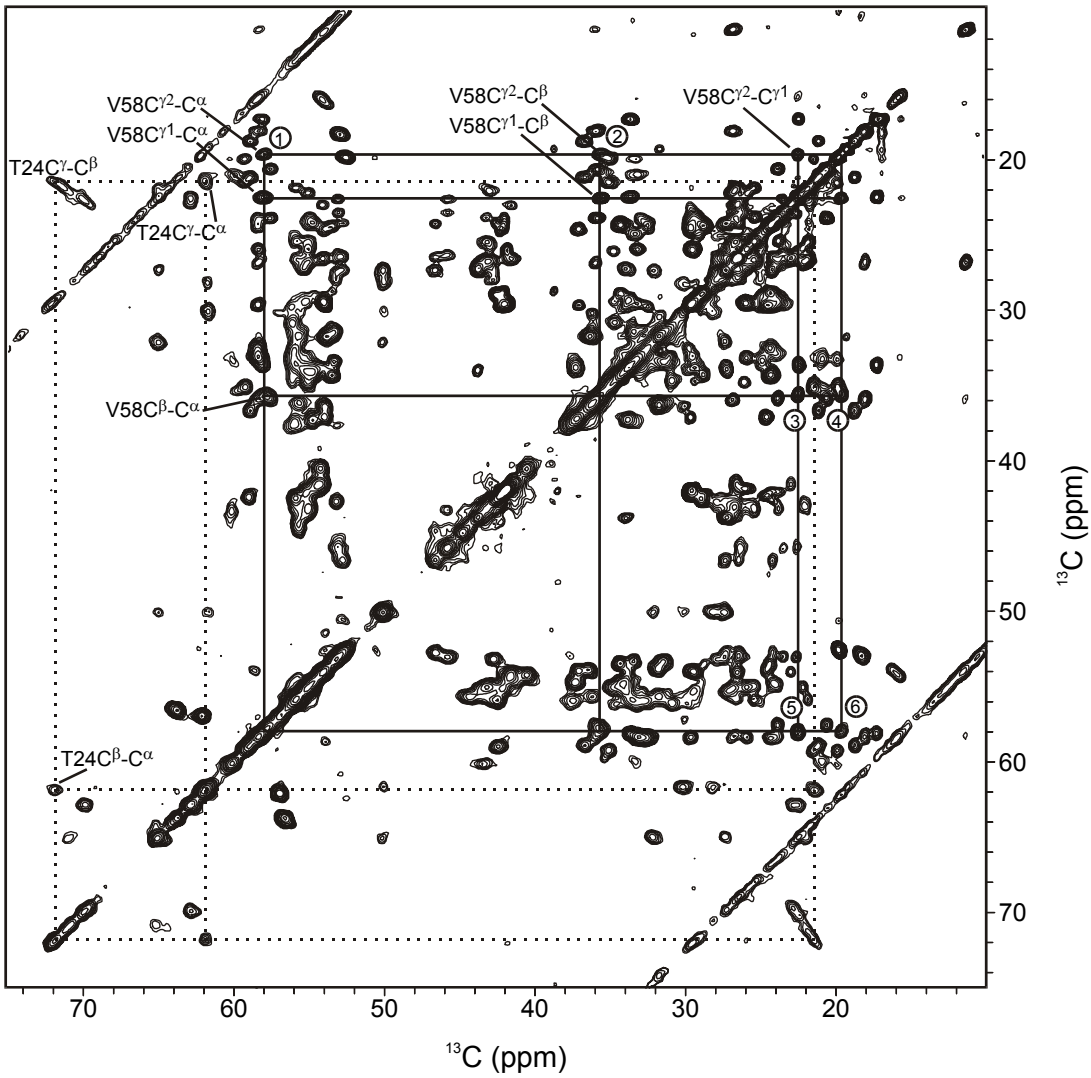

Fig. 2.2 Contour plot of a 2D ^{13}C-^{13}C RFDR dipolar correlation experiment of (U-^{15}N,^{13}C) α-spectrin SH3 domain, recorded at a field of 17.6 T, with a spinning frequency $\omega_R/2\pi = 8.0$ kHz and at a temperature of 298 K. The data were obtained using a RFDR mixing time of 3.0 ms. The lines indicate the characteristic correlation patterns of valine 58 (solid line) and threonine 24 (dashed line). The sequence specific assignment of these

residues is obtained from heteronuclear correlation experiments of the type NCA/NCO. The numbering of some correlations of V58 corresponds to the numbering of the slices of Fig. 2.6.

In the spectrum relayed-intraresidue cross-peaks were detected, that allowed the side-chain identification of almost all the residues of the protein[22]. As an example, the lines in the figure indicate correlation networks for a threonine and a valine residue.

The second step of the assignment procedure concerns the sequential assignment, that consists in correlating the side-chain signals to the backbone resonances in such a way that the sequential number can be assigned to the identified residues. For this purpose, heteronuclear ^{13}C,^{15}N correlation experiments can be recorded, that correlate the backbone nitrogen either to the neighbouring carbon of the same residue or to the carbon of the previous one. For the α-spectrin SH3 domain, experiments that selectively transfer magnetization from the amide N to the C^{α} of the same residue or the CO of the previous one were recorded, using specific ^{15}N-^{13}C cross polarization (specific-CP)[27]. These experiments are referred to as NCA and NCO. A schematic representation of the magnetization transfer in NCA and NCO experiments is shown in Fig. 2.3.

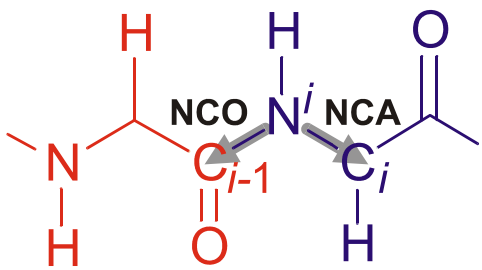

Fig. 2.3 Schematic representation of the magnetization transfer in a NCA and NCO experiments.

The experiments were extended with ^{13}C-^{13}C homonuclear exchange schemes to obtain experiments of the type NCACX and NCOCX, where 'CX' refers to any carbon. In Fig. 2.4, superimposed NCOCX (red) and NCACX (blue) spectra are shown, comprising both the carbonyl and aliphatic regions. From a combined evaluation of these spectra, it was possible to obtain the sequential assignment of the SH3 residues[22]. As an example, in the figure the correlation 'walk' from residue Q50 to V53 is shown, as well as from T37 to K39. In Appendix A, the ^{13}C and ^{15}N resonance assignment of the α-spectrin SH3 domain in the solid state is reported.

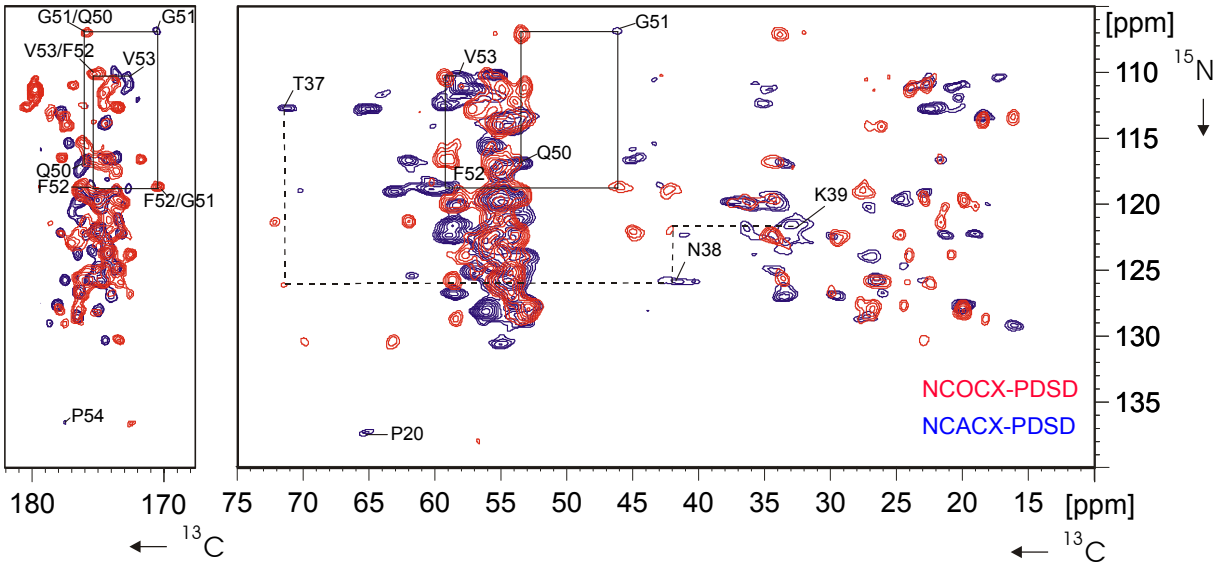

Fig. 2.4 Superposition of the NCACX-PDSD (blue) and NCOCX-PDSD (red) spectra of (U-^{15}N,^{13}C) α-spectrin SH3 domain recorded at a field of 17.6 T, with a spinning frequency $\omega_R/2\pi$ = 8.0 kHz and at a temperature of 298 K. The lines indicate the sequential assignment for the subsequence from Q50 to V53, as well as from T37 to K39.

2.3 ^{1}H resonance assignment of the α-spectrin SH3 domain

In solid-state MAS NMR, most dipolar correlation experiments for assignment and structure determination purposes are focused on ^{13}C or ^{15}N nuclei, whereas ^{1}H MAS NMR has not yet found an equally widespread application. This is due to the combined effect of the strong homonuclear dipolar interactions between the abundant protons and the small proton chemical shift dispersion, limiting the resolution in the ^{1}H spectrum. At the same time, the high abundance and gyromagnetic ratio γ of the protons offer an attractive potential for correlation spectroscopy in structural research, since proton-proton couplings are strong and magnetization can be transferred over long distances. Protons could be important for the collection of structural restraints, since they are located at the exterior of the carbon skeleton and inter-residue distances d_{CH} and d_{HH} are generally shorter than the d_{CC}. Hence, both the high-γ value and the advantageous spin topology favours the use of protons in inter-residual polarization transfer. Using the α-spectrin SH3 domain as an example, we have developed a strategy for the assignment of both the non-exchanging (section 2.3.1) and the amide protons (section 2.3.2). In appendix A, the ^{1}H resonance assignment of the α-spectrin SH3 domain in the solid-state is reported.

2.3.1 Assignment of non-exchanging proton signals

Utilising the assignment of the ^{13}C resonances of the α-spectrin SH3 domain as a starting point, the assignment of the non-exchanging protons was achieved by means of high-field 3D (^{1}H-^{13}C-^{13}C) heteronuclear dipolar correlation spectroscopy, in combination with ^{1}H homonuclear Lee-Goldburg (LG) decoupling[29]. The pulse program used for the 3D ^{1}H-^{13}C-^{13}C correlation experiment is shown in Fig. 2.5[30]. During indirect ^{1}H detection, frequency-switched LG (FSLG) is applied to significantly enhance the proton resolution. A short LG cross polarization (LGCP) mixing step of 350 μs follows, during which the protons exchange magnetization with the directly bonded carbons, while polarization transfer to remote carbons is relatively inefficient in a uniformly ^{13}C-labelled environment due to heteronuclear dipolar truncation[31] and requires longer mixing times. The ^{13}C homonuclear dipolar interactions are recoupled in the second transfer step with the RFDR technique.

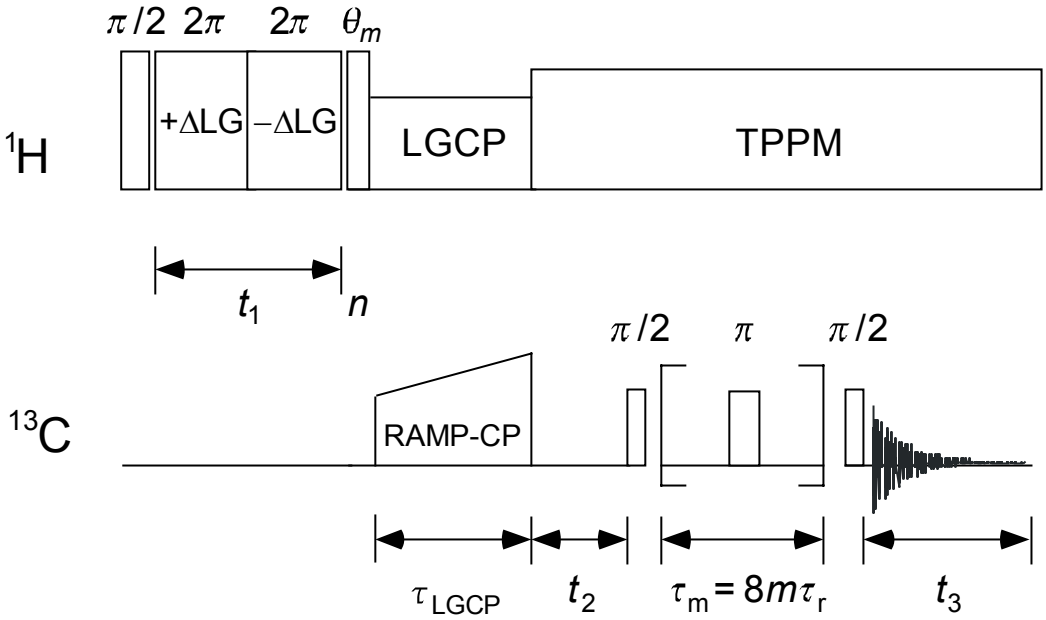

Fig. 2.5 Pulse sequence for the 3D ^{1}H-^{13}C-^{13}C heteronuclear correlation experiment used for the assignment of the non-exchanging protons of the *α*-spectrin SH3 domain. During proton evolution, FSLG is applied. Subsequently, the ^{1}H magnetization is transferred to the directly-bonded carbons via a short LGCP step of 350 μs. After the ^{13}C evolution period, the carbon magnetization is exchanged via a RFDR mixing scheme. During ^{13}C evolution and during the acquisition periods, TPPM decoupling is applied.

The assignment procedure applied to the 3D dataset is illustrated in Fig. 2.6, where several ^{1}H-^{13}C (ω_1-ω_3) slices extracted from the 3D experiment are shown as an example. The slices illustrate the assignment of the proton resonances for valine 58. The numbering of the

slices corresponds to the numbering of the correlations in Fig. 2.2 and helps to keep track of the ω_2 positions of the respective signals in the 3D spectrum. For instance, the numbers 1 and 2 in Fig. 2.2 mark the valine's correlations of the $C^{\gamma 2}$ at 19.6 ppm (ω_2) with the C^{α} and C^{β}, respectively. Slice 1 shows the corresponding $H^{\gamma 2}$-$C^{\gamma 2}$-C^{α} cross-peak in the 3D spectrum with a $^{13}C^{\alpha}$ (ω_3) shift around 57.9 ppm, while slice 2 represents the $H^{\gamma 2}$-$C^{\gamma 2}$-C^{β} correlation with an ω_3 shift of 35.6 ppm for the C^{β}. From these slices it is possible to assign the $H^{\gamma 2}$ of Val 58 unambiguously. In a similar way, the slices 3-6 provide the chemical shifts of the H^{β} and H^{α} for the selected valine.

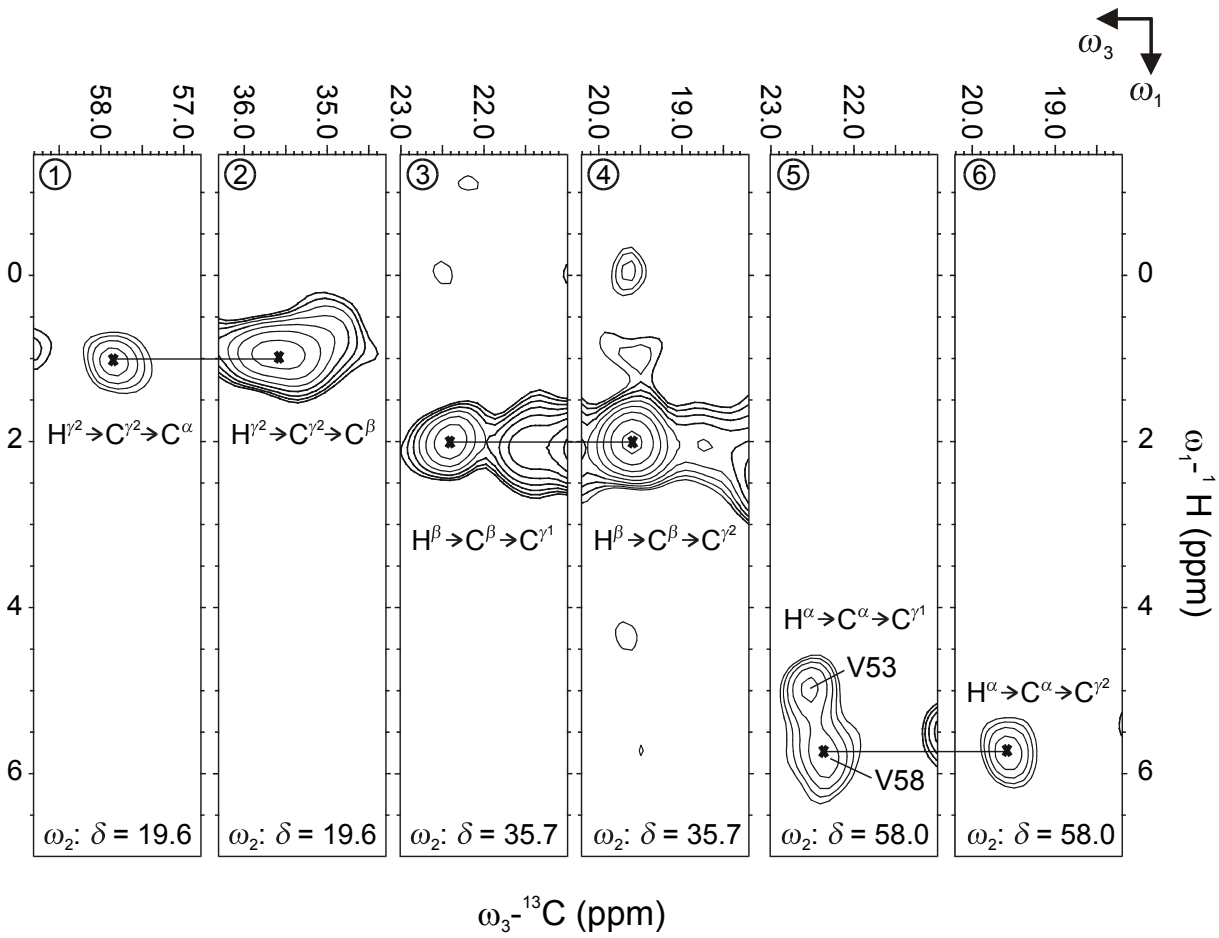

Fig. 2.6 Slices extracted from the 3D ^{1}H-^{13}C-^{13}C heteronuclear correlation experiment of (U-^{15}N,^{13}C) α-spectrin SH3 domain, recorded at a field of 17.6 T, with a spinning frequency $\omega_R/2\pi$ = 8.0 kHz and at a temperature of 298 K. The numbering of the slices corresponds to the numbering of the correlations in Fig. 2.2. The assignment of the aliphatic protons of valine 58 is illustrated.

This procedure can be repeated to assign other protons, and we were able to arrive at an almost complete assignment of the observable proton signals[30] (see Appendix A). For some residues, no solid-state NMR signal was detected with the pulse sequences employed. Among these are the residues 1-6 at the N-terminus and D62 at the C-terminus. This has been

explained in terms of the presence of multiple conformers interconverting at unfavourable rates or an interference of the increased mobility with the NMR conditions[22].

The solid-state proton assignment obtained from the 3D spectrum requires the carbon assignment as input. On the other hand, due to the additional proton dimension the overall resolution is enhanced. As a result, carbon-carbon correlations that were otherwise overlapping are now separated. An example of this improved resolution can be found in Fig. 2.6. The correlation C^{α}-$C^{\gamma 1}$ of V58 (tagged as '5') overlaps with the C^{α}-$C^{\gamma 1}$ cross-peak of V53 in the ^{13}C-^{13}C experiment. This overlap is resolved in the proton dimension of the 3D experiment, cf. slice 5 in Fig. 2.6.

2.3.2 Assignment of amide proton signals

An initial step to the assignment of the amide signals was achieved by a combined evaluation of 2D ^{1}H-^{15}N and ^{15}N-^{15}N correlation spectra[32]. Fig. 2.7a shows a contour plot of a 2D ^{1}H-^{15}N heteronuclear dipolar correlation spectrum of uniformly ^{15}N-labelled α-spectrin SH3 domain. The data were obtained at a field of 17.6 T, using PMLG ^{1}H-homonuclear decoupling during proton evolution. A cross polarization contact of 170 μs was applied to build-up heteronuclear ^{1}H-^{15}N correlations. This short contact time ensures that the spectrum is selective in the sense that only correlations between directly bonded NH pairs are observed. For these strongly coupled spin-pairs, coherent transfer leads to a rapid rise in the ^{15}N signal intensity during the first ~150 μs of the CP and results in strong correlations that contain the relevant information. In contrast, the information becomes obscured by proton spin-diffusion processes for longer mixing times (>1 ms) and the selectivity is lost, although some additional ^{15}N signal intensity may be obtained.

In Fig. 2.7b, a 2D ^{15}N correlation spectrum is shown, that was recorded at a field of 17.6 T using a standard PDSD mixing unit[33] and is used as a ruler in the assignment procedure. A long PDSD mixing time of 4.0 s was applied to exchange magnetization between the weakly coupled ^{15}N spins. In this spectrum, most of the cross-peaks are due to transfer between ^{15}N spins of sequential residues, as shown in the Fig. 2.7b for the subsequence P54 to K60. This experiment 'tells' which pairs of ^{15}N correlate and provides information about which amides are connected via sequential residues. Hence, the ^{15}N-^{15}N experiment provides an independent

check of the ^{15}N assignments, since it relies on direct transfer between the sequential ^{15}N of the protein backbone and not on a two-step transfer mechanism via the C^{α} and/or CO.

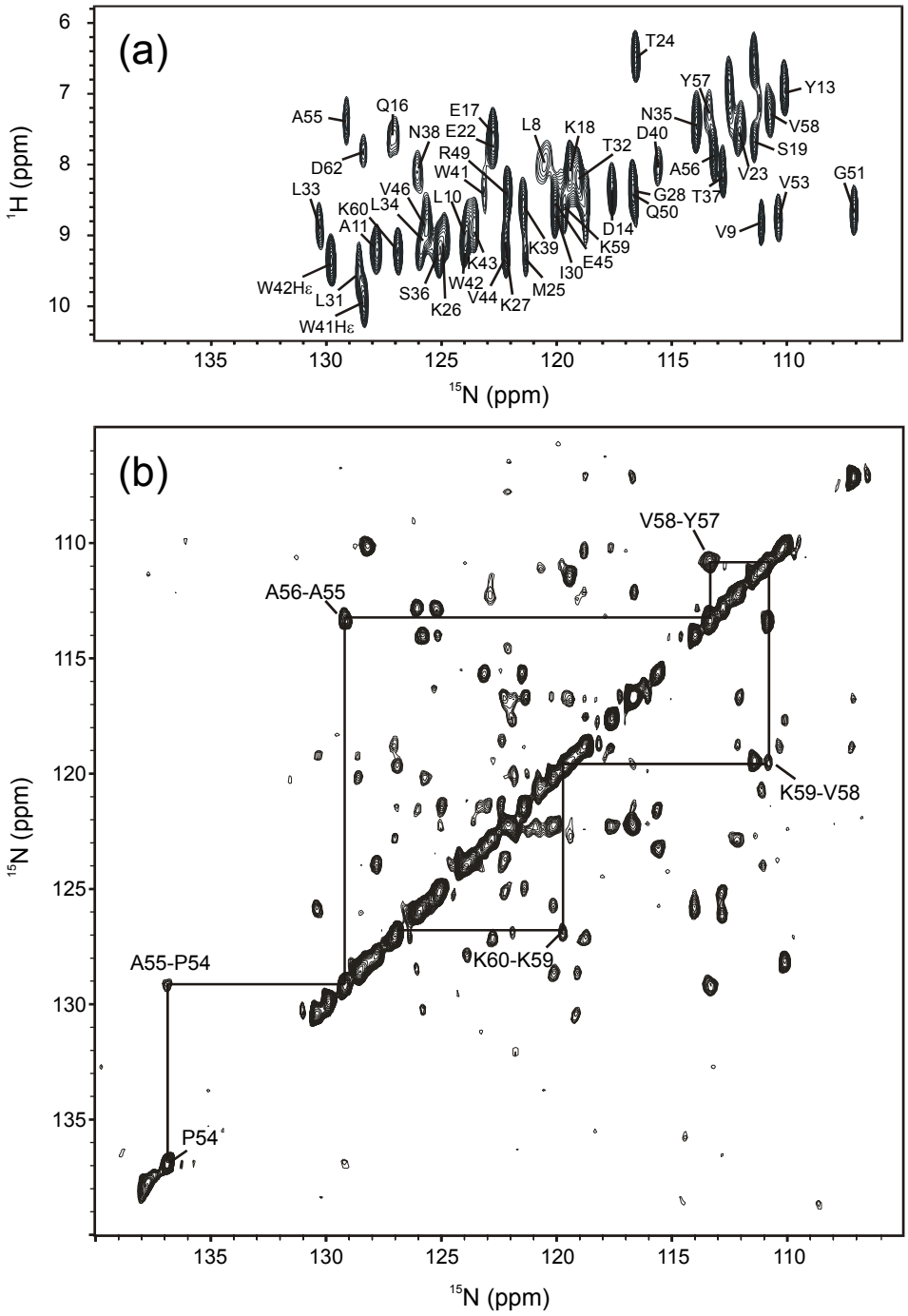

Fig. 2.7 (a) Contour plot of a 2D PMLG-decoupled ^{1}H-^{15}N heteronuclear dipolar correlation spectrum of precipitated (U-^{15}N) α-spectrin SH3 domain, recorded at a field of 17.6 T and with a spinning frequency $\omega_R/2\pi$ = 8.0 kHz. The data were obtained at a temperature of 298 K, using a short ramped CP contact of 170 µs. (b) Contour plot of a 2D ^{15}N-homonuclear dipolar correlation spectrum of precipitated (U-^{15}N) α-spectrin SH3 domain, recorded at a field of 17.6 T, with a spinning frequency $\omega_R/2\pi$ = 8.0 kHz and at a temperature of 298 K. The data were obtained using a PDSD mixing time of 4.0 s. The dashed line indicates the correlation walk from P54 to K60.

It should therefore be considered as an experiment that can be performed in parallel with the NCA(CX) and NCO(CX) experiments[22], to facilitate the assignment, and to reduce ambiguity in an early stage in the assignment procedure.

Due to the selectivity and the high resolution in the ^{15}N dimension, a large number of NH signals can be assigned unambiguously from the 2D experiment of Fig. 2.7a. There is, however, for a small number of NH pairs overlap of the ^{15}N chemical shifts, which prohibits the complete proton assignment on the basis of the 2D ^{1}H-^{15}N dataset only. Additional resolution enhancement can be achieved by exploiting the relatively well-resolved correlations in a NCA experiment. This can be done by correlating the ^{1}H-^{15}N signal with the C^{α} of the same residue in a 3D (^{1}H-^{15}N-^{13}C) heteronuclear correlation experiment (Fig. 2.8), using the pulse sequence shown in Fig. 2.9.

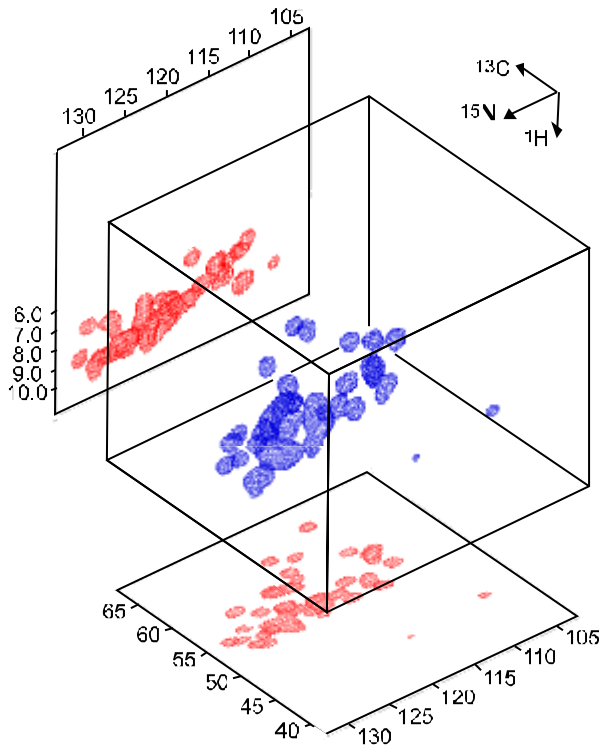

Fig. 2.8 Plot of a 3D PMLG-specific-CP HNCA correlation experiment, displayed with a single contour (blue). The 3D dataset was recorded from precipitated (U-^{15}N, ^{13}C) α-spectrin SH3 domain, at a field of 9.4 T and at a spinning frequency $\omega_R/2\pi = 8.0$ kHz. The spectrum was obtained at a temperature of 280 K. The ω_1-ω_2 (^{1}H-^{15}N) and ω_2-ω_3 (^{15}N-^{13}C) projections of the 3D experiment are shown in red.

The method combines a PMLG-decoupled ^{1}H-^{15}N experiment with specific-CP[27] following the nitrogen evolution in t_2, to transfer magnetization selectively from the backbone ^{15}N to the C^{α}. In this way, each residue gives rise to a single intra-residue $^{1}H^{N}$-^{15}N-$^{13}C^{\alpha}$ correlation in the 3D spectrum.

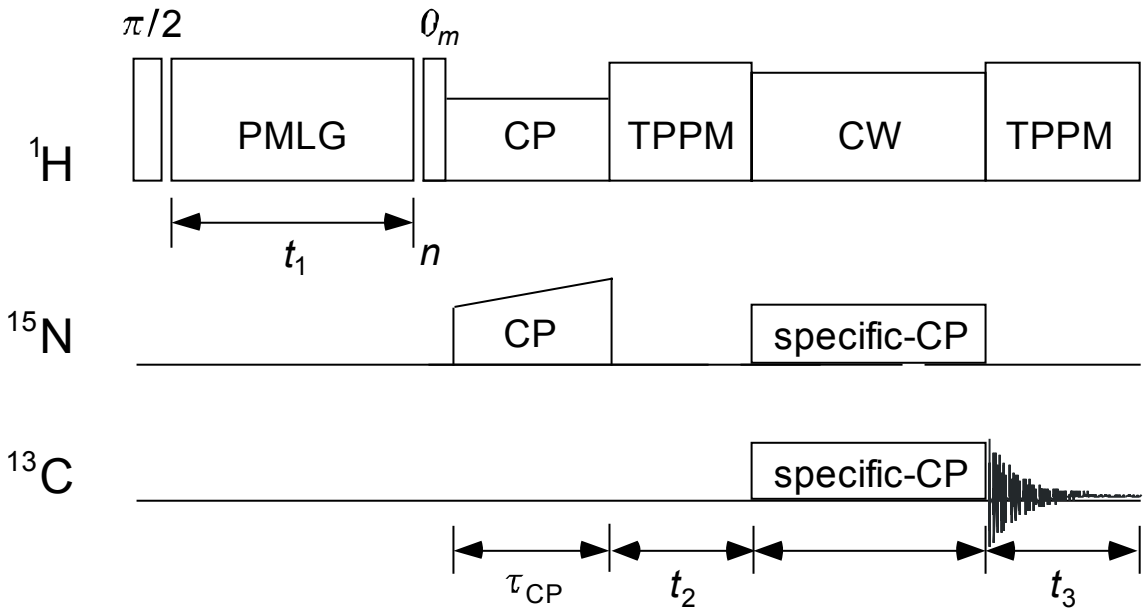

Fig. 2.9 Pulse program used for the 3D ^{1}H-^{15}N-^{13}C dipolar correlation experiment (HNCA). The ^{1}H-homonuclear dipolar interactions were suppressed with PMLG-decoupling. Heteronuclear decoupling (^{1}H-^{15}N or ^{1}H-^{13}C) was achieved with TPPM during evolution and acquisition, while continuous wave (CW) decoupling was applied during the specific-CP.

The resolution enhancement obtained in the 3D HNCA correlation experiment allows unambiguous assignments of the amide protons. This is illustrated in Fig. 2.10 for the residues T24, G28 and Q50. Fig. 2.10a shows a section of the 2D ^{1}H-^{15}N dataset in Fig. 2.7a, with the ^{15}N centred around 116.5 ppm, close to the amide ^{15}N chemical shift for the three residues. Due to overlap in the nitrogen dimension, it is not possible to assign the amide protons of T24, G28 and Q50 unambiguously from the 2D experiment. On the other hand, the C$^{\alpha}$ resonate with different chemical shifts for T24, Q50 and G28, at 61.9 ppm, 53.4 ppm and 45.1 ppm, respectively. Hence the signals from the three residues are fully resolved in the NCA dimension of the experiment (cf. Fig. 2.10b and c) and the three amide protons can be assigned unambiguously from the ω_1-ω_3 slice extracted from the 3D dataset with an ω_2 ^{15}N shift near 116.6 ppm (Fig. 2.10b). In this way, all ^{1}H^{N} shifts could be assigned unambiguously, using the combined 2D and 3D datasets (see Appendix A). The ^{1}H^{N} that we could not detect are from the first seven residues on the N-terminus (M1-E7), and from the residues N47 and D48.

The ^{1}H^{N} assignment forms an important fist step for the use of the amides in structural research. NH groups are important structural monitors, since they are often involved in the formation of hydrogen-bonds that stabilise the folding of a protein. In addition, the NH

chemical shifts are sensitive to the protein backbone conformations, therefore providing secondary structure information. In MAS NMR, amide ^{1}H and ^{15}N nuclei may be used for the detection of N-H···X bond lengths, for the measurement of torsion angles or of HH distance restraints[34-40]. In particular, for the detection of long-range H-H correlations, the amide protons are potentially useful due to their high-γ, once samples that are perdeutarated at the non-exchangeable sites are provided. Perdeuteration removes all strong ^{1}H-^{1}H dipolar couplings and leads to relatively well-resolved proton spectra, while applying mild ^{1}H-homonuclear decoupling. This makes a semi-quantitative analysis of transfer events and cross-peak intensities feasible[41].

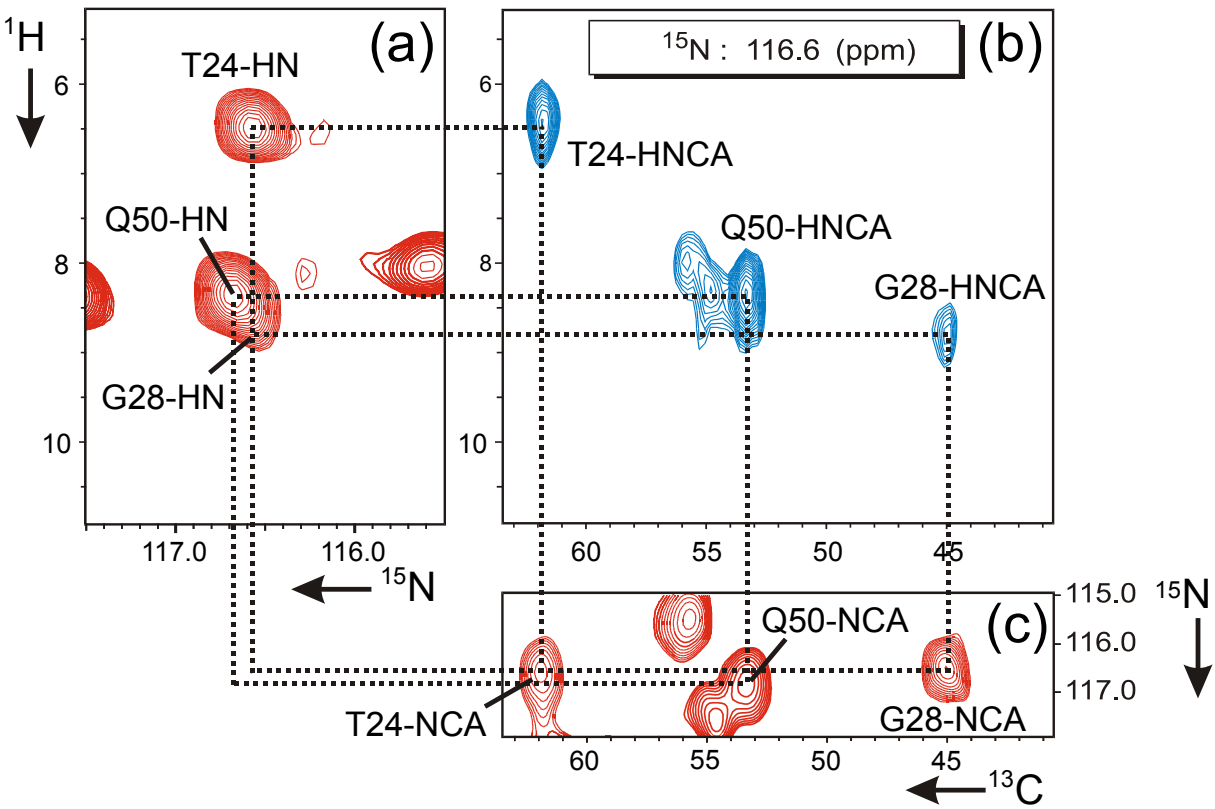

Fig. 2.10 Assignment of the amides of T24, G28 and Q50. (a) shows a section of the 2D ^{1}H-^{15}N experiment of Fig. 2.7a, centred around the ^{15}N chemical shift of the three residues (~116.6 ppm). In (b), a plane from the 3D HNCA dataset is shown, extracted at the same ^{15}N chemical shift. Finally, (c) shows a strip from a 2D NCA experiment, recorded from (U-^{15}N, ^{13}C) α-spectrin SH3 domain at a field of 9.4 T and using a spinning frequency $\omega_R/2\pi = 8.0$ kHz.

2.4 Materials and methods

2.4.1 Sample preparation

The SH3 protein was expressed in *Escherichia coli* BL21 (DE3), using M9 minimal media. Plasmid pET3d coding for α-spectrin SH3 protein from chicken brain was a generous gift of Dr. M. Saraste (EMBL, Heidelberg). For (U-^{13}C,^{15}N)-SH3, 1.5 g of [U-^{13}C] glucose and 1.0 g $^{15}NH_4Cl$ per litre of medium were added[20]. The proteins were purified by anion exchange chromatography (Q-Sepharose FF, Amersham Pharmacia Biotech), gel filtration (Superdex 75 pg, Amersham Pharmacia Biotech) and dialysis. The final yield was approximately 20 mg of protein per litre of culture. A 200 mM $(NH_4)_2SO_4$ solution (pH 3.5, 0.04% NaN_3) was added to a 1.15 mM SH3 solution (pH 3.5) at a volume ratio of 1:1. The protein samples for MAS measurement were precipitated by changing the pH to a value of 7.5 in NH3 atmosphere. The solution was kept in a refrigerator (4ºC) overnight before the precipitate was separated and centrifuged inside 4-mm CRAMPS rotors at 15000 g. For the MAS measurements, approximately 6-7 mg of protein was used and confined to the centre of 4 mm rotors by use of spacers.

2.4.2 Solid-state NMR spectroscopy

Experimental details for the 2D ^{13}C-^{13}C RFDR dipolar correlation experiment and the triple-resonance NCACX and NCOCX spectra are described by Pauli et al.[22].

The 3D (^{1}H-^{13}C-^{13}C) heteronuclear dipolar correlation spectrum was recorded at a field of 17.6 T on a DMX-750 spectrometer, equipped with a 4mm double-resonance CP/MAS probe (Bruker, Karlsruhe, Germany), The data were collected at ambient temperature and at a MAS frequency $\omega_R/2\pi$ = 8.0 kHz. For the FSLG decoupling[16,17], a proton RF power of 102 kHz was used, which corresponds to an effective LG nutation frequency of 125 kHz. Prior to the experiments, the efficiency of the FSLG decoupling was optimized on a preparation of natural abundance adamantane. This was done by observing the J_{CH}-couplings in 1D ^{13}C spectra collected with FSLG irradiation during data acquisition, and by fine-tuning of the LG offset frequencies and appropriate timing of delays to yield optimally resolved doublet and triplet line shapes for the CH and CH_2 moieties, respectively. The resultant offset frequencies

are about 5 % higher than the values calculated from the ^{1}H nutation frequency. A slight increase of the offset frequency above a LG condition generally results in a more favorable scaling factor, while the additional line broadening as the consequence of a slight deviation from optimal LG irradiation is only very moderate. The cross polarization unit contained a ramped spin-lock pulse on the carbon nuclei to broaden the CP matching profile at high MAS frequencies[42]. Selective heteronuclear polarization transfer was achieved using LGCP[43,44]. A moderate proton RF power corresponding to a ^{1}H nutation frequency of 48 kHz was applied for the LGCP. Proton decoupling was achieved by use of the two-pulse phase modulation (TPPM) decoupling scheme[45] during ^{13}C acquisition, ^{13}C evolution and mixing periods. A pulse length of 7.0 μs and a phase modulation angle of 20 degrees were used for the TPPM decoupling. The exchange of polarization through homonuclear ^{13}C dipolar interactions during τ_m was promoted by the use of an integral multiple of XY-8 phase-alternated rotor-synchronized trains of π-pulses as described previously[46]. Low power ^{13}C π-pulses of ~23 μs were applied to avoid signal losses due to unwanted CP during the carbon recoupling. A short LGCP contact time of 350 μs was used to minimize ^{1}H homonuclear coherence exchange during CP, while the RFDR mixing time was kept relatively short (2.0 ms) to avoid exchange of proton modulation via recoupling of the carbon spins.

The 2D ^{1}H-^{15}N and ^{15}N-^{15}N dipolar correlation experiments were performed at 298 K at a field of 17.6 T using a wide-bore DMX-750 spectrometer (Bruker, Karlsruhe, Germany). The 3D ^{1}H-^{15}N-^{13}C dataset was recorded at 280 K, with a DMX-400 spectrometer operating at a field of 9.4 T (Bruker, Karlsruhe, Germany). Both spectrometers were equipped with 4mm triple-resonance CP/MAS probes (Bruker, Karlsruhe, Germany). The ^{1}H-^{15}N dipolar correlation experiment employs phase-modulated Lee-Goldburg (PMLG) irradiation during proton evolution to suppress strong ^{1}H-homonulear dipolar interactions[18]. For the ^{15}N-homonuclear correlation experiment, a standard PDSD sequence was used, with a mixing time of 4.0 s[33]. The 3D ^{1}H-^{15}N-^{13}C experiment is shown in Fig. 2.9 and applies specific-CP[27] to transfer magnetization selectively between the amide ^{15}N and the $^{13}C^{\alpha}$ of the same residue. For PMLG decoupling a shaped-pulse was used that mimics each frequency offset with a phase trajectory that contains three phase steps (PMLG-3)[47]. The shaped pulse contains 2048 complete PMLG cycles and has a total duration τ_{tot}. The efficiency of the PMLG decoupling was optimised using the natural abundance ^{13}C signals of adamantane, as explained above. The proton evolution in t_1 was sampled at intervals τ_{inc} corresponding to two complete PMLG

cycles (typically 40 μs). The increment τ_{inc} was first calculated according to $\tau_{tot}/1024$, rounded off to the nearest integral multiple of 100 ns. Subsequently, τ_{tot} was recalculated as ($\tau_{inc}\cdot 1024$). This was done to ensure synchronization of $n\cdot\tau_{inc}$ with the shaped pulse for large n. For similar reasons, the starting increment for the indirect detection can not be chosen arbitrarily, but should be set to 0 μs or to a small multiple of $\tau_{inc}/2$. The PMLG decoupling was optimised for the SH3 preparations by adjusting the ^{1}H RF strength to yield similar ^{1}H pulse lengths as found for the adamantane sample. For all SH3 samples that we have studied, this results in RF powers that are about 10% higher than for adamantane. The protons were decoupled by use of the two-pulse phase modulation (TPPM) decoupling scheme during all acquisition periods and during the indirect ^{15}N evolution in the correlation experiments[45]. The TPPM decoupling was optimised directly on the SH3 domain preparations, yielding pulse lengths of typically 7.0 μs for a phase modulation angle of 15 degrees. For the specific-CP, RF powers corresponding to nutation frequencies of ~15 kHz (^{15}N) and ~20 kHz (^{13}C) were applied. The amide ^{15}N were irradiated close to resonance and the C^{α} off-resonance. The ^{13}C offset was optimised for maximal C^{α} signal, using a 1D version of the pulse program.

All the solid-state data were processed with the XWINNMR software, version 2.6 (Bruker, Karlsruhe, Germany) and subsequently analysed using the program Sparky, version 3.100 (T.D. Goddard & D.G. Kneller, University of California).

References

1. Wagner, G. & Wuthrich, K. (1982). Sequential resonance assignments in protein 1H nuclear magnetic resonance spectra. Basic pancreatic trypsin inhibitor. *J. Mol. Biol.* **155**, 347-366.

2. Clore, G. M. & Gronenborn, A. M. (1991). Applications of 3-Dimensional and 4-Dimensional Heteronuclear Nmr-Spectroscopy to Protein-Structure Determination. *Prog. Nucl. Magn. Reson. Spectrosc.* **23**, 43-92.

3. Grzesiek, S. & Bax, A. (1992). An Efficient Experiment for Sequential Backbone Assignment of Medium-Sized Isotopically Enriched Proteins. *J. Magn. Reson.* **99**, 201-207.

4. Bax, A. (1994). Multidimensional Nuclear-Magnetic-Resonance Methods for Protein Studies. *Curr. Opin. Struct. Biol.* **4**, 738-744.

5. Ernst, R. R., Bodenhausen, G., & Wokaun, A. (2002). *Principles of Nuclear Magnetic Resonance in One and Two Dimensions* Clarendon Press, Oxford.

6. Cavanagh, J., Fairbrother, W. J., Palmer III, A. G., & Skelton, N. J. (1996). *Protein NMR Spectroscopy: Principles and Practice* Academic Press, San Diego CA.

7. Fiaux, J., Bertelsen, E. B., Horwich, A. L., & Wuthrich, K. (2002). NMR analysis of a 900K GroEL-GroES complex. *Nature* **418**, 207-211.

8. Bennett, A. E., Ok, J. H., Griffin, R. G., & Vega, S. (1992). Chemical-Shift Correlation Spectroscopy in Rotating Solids - Radio Frequency-Driven Dipolar Recoupling and Longitudinal Exchange. *J. Chem. Phys.* **96**, 8624-8627.

9. Baldus, M., Tomaselli, M., Meier, B. H., & Ernst, R. R. (1994). Broad-Band Polarization-Transfer Experiments for Rotating Solids. *Chem. Phys. Lett.* **230**, 329-336.

10. Sun, B. Q., Costa, P. R., Kocisko, D., Lansbury, P. T., & Griffin, R. G. (1995). Internuclear Distance Measurements in Solid-State Nuclear-Magnetic-Resonance - Dipolar Recoupling Via Rotor Synchronized Spin Locking. *J. Chem. Phys.* **102**, 702-707.

11. Gregory, D. M., Mitchell, D. J., Stringer, J. A., Kiihne, S., Shiels, J. C., Callahan, J., Mehta, M. A., & Drobny, G. P. (1995). Windowless Dipolar Recoupling - the Detection of Weak Dipolar Couplings Between Spin-1/2 Nuclei with Large Chemical-Shift Anisotropies. *Chem. Phys. Lett.* **246**, 654-663.

12. Lee, Y. K., Kurur, N. D., Helmle, M., Johannessen, O. G., Nielsen, N. C., & Levitt, M. H. (1995). Efficient Dipolar Recoupling in the Nmr of Rotating Solids - A Sevenfold Symmetrical Radiofrequency Pulse Sequence. *Chem. Phys. Lett.* **242**, 304-309.

13. Hohwy, M., Jakobsen, H. J., Eden, M., Levitt, M. H., & Nielsen, N. C. (1998). Broadband dipolar recoupling in the nuclear magnetic resonance of rotating solids: A compensated C7 pulse sequence. *J. Chem. Phys.* **108**, 2686-2694.

14. Rienstra, C. M., Hatcher, M. E., Mueller, L. J., Sun, B. Q., Fesik, S. W., & Griffin, R. G. (1998). Efficient multispin homonuclear double-quantum recoupling for magic-angle spinning NMR: C-13-C-13 correlation spectroscopy of U-C-13-erythromycin A. *J. Am. Chem. Soc.* **120**, 10602-10612.

15. Hohwy, M., Rienstra, C. M., Jaroniec, C. P., & Griffin, R. G. (1999). Fivefold symmetric homonuclear dipolar recoupling in rotating solids: Application to double quantum spectroscopy. *J. Chem. Phys.* **110**, 7983-7992.

16. Bielecki, A., Kolbert, A. C., & Levitt, M. H. (1989). Frequency-Switched Pulse Sequences - Homonuclear Decoupling and Dilute Spin Nmr in Solids. *Chem. Phys. Lett.* **155**, 341-346.

17. vanRossum, B. J., Forster, H., & deGroot, H. J. M. (1997). High-field and high-speed CP-MAS C-13 NMR heteronuclear dipolar-correlation spectroscopy of solids with frequency-switched Lee-Goldburg homonuclear decoupling. *J. Magn. Reson.* **124**, 516-519.

18. Vinogradov, E., Madhu, P. K., & Vega, S. (1999). High-resolution proton solid-state NMR spectroscopy by phase-modulated Lee-Goldburg experiment. *Chem. Phys. Lett.* **314**, 443-450.

19. Hafner, S. & Spiess, H. W. (1996). Multiple-pulse line narrowing under fast magic-angle spinning. *J. Magn. Reson. A* **121**, 160-166.

20. Pauli, J., van Rossum, B., Forster, H., de Groot, H. J. M., & Oschkinat, H. (2000). Sample optimization and identification of signal patterns of amino acid side chains in 2D RFDR spectra of the alpha-spectrin SH3 domain. *J. Magn. Reson.* **143**, 411-416.

21. McDermott, A., Polenova, T., Bockmann, A., Zilm, K. W., Paulson, E. K., Martin, R. W., Montelione, G. T., & Paulsen, E. K. (2000). Partial NMR assignments for uniformly (13C, 15N)-enriched BPTI in the solid state. *J. Biomol. NMR* **16**, 209-219.

22. Pauli, J., Baldus, M., van Rossum, B., de Groot, H., & Oschkinat, H. (2001). Backbone and side-chain C-13 and N-15 signal assignments of the alpha-spectrin SH3 domain by magic angle spinning solid-state NMR at 17.6 tesla. *Chembiochem* **2**, 272-281.

23. Egorova-Zachernyuk, T. A., Hollander, J., Fraser, N., Gast, P., Hoff, A. J., Cogdell, R., de Groot, H. J., & Baldus, M. (2001). Heteronuclear 2D-correlations in a uniformly [13C, 15N] labeled membrane-protein complex at ultra-high magnetic fields. *J. Biomol. NMR* **19**, 243-253.

24. Hong, M. (1999). Resonance assignment of 13C/15N labeled solid proteins by two- and three-dimensional magic-angle-spinning NMR. *J. Biomol. NMR* **15**, 1-14.

25. Straus, S. K., Bremi, T., & Ernst, R. R. (1998). Experiments and strategies for the assignment of fully 13C/15N-labelled polypeptides by solid state NMR. *J. Biomol. NMR* **12**, 39-50.

26. Kiihne, S., Mehta, M. A., Stringer, J. A., Gregory, D. M., Shiels, J. C., & Drobny, G. P. (1998). Distance measurements by dipolar recoupling two-dimensional solid-state NMR. *Journal of Physical Chemistry A* **102**, 2274-2282.

27. Baldus, M., Petkova, A. T., Herzfeld, J., & Griffin, R. G. (1998). Cross polarization in the tilted frame: assignment and spectral simplification in heteronuclear spin systems. *Mol. Phys.* **95**, 1197-1207.

28. Gullion, T. & Schaefer, J. (1989). Rotational-Echo Double-Resonance Nmr. *J. Magn. Reson.* **81**, 196-200.

29. Lee, M. & Goldburg, W. I. (1965). *Phys. Rev. A* **140**, 1261-1271.

30. van Rossum, B. J., Castellani, F., Rehbein, K., Pauli, J., & Oschkinat, H. (2001). Assignment of the nonexchanging protons of the alpha-spectrin SH3 domain by two- and three-dimensional H-1-C-13 solid-state magic-angle spinning NMR and comparison of solution and solid-state proton chemical shifts. *Chembiochem* **2**, 906-914.

31. Ladizhansky, V., Vinogradov, E., van Rossum, B. J., de Groot, H. J. M., & Vega, S. (2003). Multiple-spin effects in fast magic angle spinning Lee-Goldburg cross-polarization experiments in uniformly labeled compounds. *J. Chem. Phys.* **118**, 5547-5557.

32. van Rossum, B. J., Castellani, F., Pauli, J., Rehbein, K., Hollander, J., de Groot, H. J., & Oschkinat, H. (2003). Assignment of amide proton signals by combined evaluation of HN, NN and HNCA MAS-NMR correlation spectra. *J. Biomol. NMR* **25**, 217-223.

33. Szeverenyi, N. M., Sullivan, M. J., & Maciel, G. E. (1982). Observation of Spin Exchange by Two-Dimensional Fourier-Transform C-13 Cross Polarization-Magic-Angle Spinning. *J. Magn. Reson.* **47**, 462-475.

34. Brown, S. P., Zhu, X. X., Saalwachter, K., & Spiess, H. W. (2001). An investigation of the hydrogen-bonding structure in bilirubin by 1H double-quantum magic-angle spinning solid-state NMR spectroscopy. *J. Am. Chem. Soc.* **123**, 4275-4285.

35. Hohwy, M., Jaroniec, C. P., Reif, B., Rienstra, C. M., & Griffin, R. G. (2000). Local structure and relaxation in solid-state NMR: Accurate measurement of amide N-H bond lengths and H-N-H bond angles. *J. Am. Chem. Soc.* **122**, 3218-3219.

36. Hong, M., Gross, J. D., & Griffin, R. G. (1997). Site-resolved determination of peptide torsion angle phi from the relative orientations of backbone N-H and C-H bonds by solid-state NMR. *J. Phys. Chem. B* **101**, 5869-5874.

37. Reif, B., Hohwy, M., Jaroniec, C. P., Rienstra, C. M., & Griffin, R. G. (2000). NH-NH vector correlation in peptides by solid-state NMR. *J. Magn. Reson.* **145**, 132-141.

38. Schnell, I., Brown, S. P., Low, H. Y., Ishida, H., & Spiess, H. W. (1998). An investigation of hydrogen bonding in benzoxazine dimers by fast magic-angle spinning and double-quantum H-1 NMR spectroscopy. *J. Am. Chem. Soc.* **120**, 11784-11795.

39. Zhao, X., Sudmeier, J. L., Bachovchin, W. W., & Levitt, M. H. (2001). Measurement of NH bond lengths by fast magic-angle spinning solid-state NMR spectroscopy: a new method for the quantification of hydrogen bonds. *J. Am. Chem. Soc.* **123**, 11097-11098.

40. Song, X. & McDermott, A. E. (2001). Proton transfer dynamics and N-H bond lengthening in N-H N model systems: a solid-state NMR study. *Magn. Reson. Chem.* **39**, 37-43.

41. Reif, B., van Rossum, B. J., Castellani, F., Rehbein, K., Diehl, A., & Oschkinat, H. (2003). Characterization of (1)H-(1)H Distances in a Uniformly (2)H,(15)N-Labeled SH3 Domain by MAS Solid-State NMR Spectroscopy(section sign). *J. Am. Chem. Soc.* **125**, 1488-1489.

42. Metz, G., Wu, X. L., & Smith, S. O. (1994). Ramped-Amplitude Cross-Polarization in Magic-Angle-Spinning Nmr. *J. Magn. Reson. A* **110**, 219-227.

43. Caravatti, P., Bodenhausen, G., & Ernst, R. R. (1982). Heteronuclear Solid-State Correlation Spectroscopy. *Chem. Phys. Lett.* **89**, 363-367.

44. Wu, C. H., Ramamoorthy, A., & Opella, S. J. (1994). High resolution heteronuclear dipolar solid-state NMR spectroscopy. *J. Magn. Reson. A* **109**, 270-272.

45. Bennett, A. E., Rienstra, C. M., Auger, M., Lakshmi, K. V., & Griffin, R. G. (1995). Heteronuclear decoupling in rotating solids. *J. Chem. Phys.* **103**, 6951-6958.

46. Boender, G. J., Raap, J., Prytulla, S., Oschkinat, H., & deGroot, H. J. M. (1995). Mas Nmr Structure Refinement of Uniformly C-13 Enriched Chlorophyll-A Water Aggregates with 2D Dipolar Correlation Spectroscopy. *Chem. Phys. Lett.* **237**, 502-508.

47. Vinogradov, E., Madhu, P. K., & Vega, S. (1999). *Chem. Phys. Lett.* **314**, 443.